Triple-negative breast cancer cells that survive ionizing radiation exhibit an Axl-dependent aggressive radioresistant phenotype

JIANFENG JI[1], YUQIN DING[2], YUE KONG[3], MIN FANG[3], XIAOFU YU[3], XIAOJING LAI[3] and QING GU[3]

Departments of [1]Nuclear Medicine, [2]Breast Surgery and [3]Radiation Oncology, Zhejiang Cancer Hospital, Institute of Basic Medicine and Cancer, Chinese Academy of Sciences, Hangzhou, Zhejiang 310022, P.R. China

Received April 13, 2023; Accepted July 10, 2023

DOI: 10.3892/etm.2023.12147

Abstract. This study aimed to investigate the aggressive behavior of triple-negative breast cancer (TNBC) cells that had survived ionizing radiation and explore the potential targets of TNBC combination treatment. Consistent with the previous literature, Axl was highly expressed in TNBC and closely associated with the degree of malignancy based on immunohistochemical staining. Using a gradient irradiation method, the ionizing radiation-resistant mouse TNBC cell line 4T-1/IRR was established. It was found that Axl expression was upregulated in 4T-1/IRR cells. After irradiation by X-ray, the cell viability and colony formation ability of 4T-1/IRR cells were significantly increased when compared with the 4T-1 cells. Combined radiotherapy with Axl inhibition by treatment with R428 and small interfering RNA lentivirus targeting Axl infection significantly reduced cell viability, colony formation ability, DNA double-stranded break repair, and the invasive and migratory ability of 4T-1/IRR cells. *In vivo*, the small animal radiation research platform was applied to precisely administer radiotherapy of the tumor-bearing mice. R428 treatment combined with 6 Gy X-ray significantly inhibited the growth of 4T-1/IRR cells-derived xenograft tumors in the BALB/c mouse. The results of western blotting showed that the critical molecular mechanism involved in the radioresistance of TNBC cells was the PI3K/Akt/mTOR signaling pathway induced by Axl activation. Thus, it is hypothesized that targeted Axl therapy combined with radiotherapy may have significant potential for the treatment of TNBC.

Correspondence to: Dr Qing Gu or Dr Xiaojing Lai, Department of Radiation Oncology, Zhejiang Cancer Hospital, Institute of Basic Medicine and Cancer, Chinese Academy of Sciences, 1 East Banshan Road, Hangzhou, Zhejiang 310022, P.R. China
E-mail: guqing@zjcc.org.cn
E-mail: laixj@zjcc.org.cn

Key words: Axl, PI3K, Akt, triple negative breast cancer, Ionizing radiation resistance

Introduction

Triple-negative breast cancer (TNBC) is an aggressive disease with a high incidence of recurrence and metastasis, which often exhibits therapeutic resistance, and is associated with poor survival outcomes. Tumor recurrence is one of the primary causes of failure of radiotherapy, and cells that survive radiotherapy often exhibit rapid proliferative rates (1-3). A series of genetic and epigenetic disturbances are reported to be involved in the radioresistance mechanisms of tumor cells (4,5). Therefore, research on specific molecular targets and the tumor immune microenvironment is gradually resulting in advances in malignant tumor treatment regimens (6,7). Combination therapy of traditional therapies with targeted drugs or immune checkpoint inhibitors has seen increased popularity for the management of malignant tumors.

Receptor tyrosine kinases (RTKs) are the most widespread type of enzyme-linked receptors in humans and include the EGFR family and the VEGFR family, which are widely targeted in clinical practice. By binding to ligands, RTKs induce the phosphorylation of tyrosine residues of downstream target proteins, causing downstream intracellular effects, and play an important role in the occurrence and development of various types of malignant tumors (8). Axl is a transmembrane protein belonging to the TAM (TYRO3, AXL, and MERTK) family of RTKs. Following the binding and activation by extracellular ligands, the conformation of Axl is altered to form homodimers or heterodimers. Phosphorylation of tyrosine residues in the intracellular domain activates the kinase activity and induces signaling cascades, including the JAK/STAT, PI3K/Akt, RAS/RAF/MEK/ERK, and NF-κB signaling pathways, which are widely involved in various biological processes such as tissue generation, cell proliferation, cellular adhesion and recognition, inhibition of apoptosis, malignant transformation, and treatment resistance (9).

In recent years, various studies have shown that Axl overexpression is closely associated with drug resistance to targeted therapy, chemotherapy, and immunotherapy. Previous studies have found that mouse breast cancer tumors with high Axl expression exhibit resistance to combination therapy consisting of ionizing radiation and immune checkpoint inhibitors. Inhibition of Axl expression enhances antigen presentation, affects cytokine secretion, regulates immune response in tumors, and ultimately increases the lethality of

radiotherapy (10). When drugs target malignant tumors, the phosphorylation of Axl is also upregulated, followed by the activation of the downstream cell survival signaling pathways, and this eventually leads to treatment resistance (11). Inhibition of Axl expression or its phosphorylation reduces cell proliferation and migration while maintaining therapeutic drug sensitivity (12-15).

Previous studies have shown that Axl activation promotes the expression of anti-apoptotic proteins, inhibits the expression of pro-apoptotic proteins, and ultimately promotes cell survival by activating the downstream PI3K/Akt signaling pathway (16,17). It can also induce the expression of matrix metalloproteins (MMPs), degrade the extracellular matrix, and promote the invasion and migration of tumor cells (16,18-20). The activation of the PI3K pathway induces the phosphorylation of Akt and mTOR, leading to an increase in the proliferation of breast cancer cells and the occurrence of distant metastasis (21).

Ionizing radiation induces a series of survival-promoting signaling pathways whilst destroying a tumor. The activation of the PI3K/Akt signaling pathway following exposure of malignant tumors to ionizing radiation is often observed (22). The activation of the PI3K/Akt signaling pathway usually indicates the resistance of tumor cells to ionizing radiation. Inhibiting the activation of the PI3K/Akt signaling pathway increases the radiosensitivity of various malignant tumor cells, and the potential mechanism may be associated with the inhibition of DNA damage repair and increased cell apoptosis (23).

In the present study, the radioresistance of the TNBC cells that had survived ionizing radiation was investigated, and the potential value of targeting Axl combined with radiotherapy in the treatment of TNBC is discussed.

Materials and methods

Tumor tissues and immunohistochemistry. A total of 45 surgical resection specimens (including cancer tissue and paracancerous tissue) of primary TNBC were collected from the biological sample bank of Zhejiang Cancer Hospital (Zhejiang, China). The median age (range) at diagnosis was 56 years (37 to 69). The paracancerous tissue was at least 2 cm away from the edge of the tumor tissue. The clinical data of the specimens were obtained from the medical records of the hospital. Immunohistochemistry was used to detect the expression of Axl in TNBC tissues and adjacent paracancerous tissues, as well as the expression of pAkt in cancerous tissues. The study protocol was approved by the Ethics Committee of Zhejiang cancer hospital (approval no, IRB-2020-367). For statistical analysis, the degree of positive staining was classified as negative (0), weakly positive (+), moderately positive (++), and strongly positive (+++), corresponding to the tissues with <10%, 10-25%, 25-75% and >75% of the tissue stained positive, respectively.

Cell culture and treatment. The mouse TNBC cell line 4T-1 was purchased from the ATCC cell bank represented by the Beijing Beina Chuanglian Institute of Biotechnology (cat. no. BNCC273810). Cells were maintained in RPMI-1640 Medium (HyClone; Cytiva), supplemented with 10% FBS (Gibco; Thermo Fisher Scientific, Inc.) and 100 U/ml penicillin, and 100 μg/ml streptomycin (Biosharp, Inc.) and maintained in a humidified incubator at 37˚C supplied with 5% CO_2 air. R428 was purchased from APExBIO Technology and dissolved in PBS (HyClone; Cytiva).

Establishment of the ionizing radiation-resistant cell line. The 4T-1 cells resistant to ionizing radiation (henceforth referred to as 4T-1/IRR) were established using a gradient irradiation method. 4T-1 cells in the logarithmic growth phase were cultured in a 25 cm^2 culture flask and irradiated using a 2 Gy X-ray initially. Cells were passaged and irradiated again with 2 Gy X-ray when the cell density reached 80-90%. The aforementioned 4T-1 cells were irradiated by gradually increasing doses to 4, 6, 8, and finally 10 Gy, with cells being irradiated with each dose twice, such that the total irradiation dose was 60 Gy. After continued culturing and passaging for 15 days after each irradiation treatment, a few of the cells survived and proliferated stably. An MTT assay and colony formation assay were used to identify ionizing radiation-resistant cell lines.

Lentiviral infection. Cell suspension with a density of 3-5x10^4 cells/ml was prepared by RPMI-1640 complete medium. Then 6-10x10^4 cells in 2 ml cell suspension were inoculated into each well of 6-well plates and incubated for 16-24 h to 20-30% confluency as above. The small interfering RNA (siRNA) sequences used were as follows: siAxl, TGT CTGCATGAAGGAATTT and NC, TTCTCCGAACGTGTC ACGT. During lentiviral infection, the volume of serum-free medium in each well of the six-well plate was 1 ml; 40 μl HiTransG A infection reagent (Shanghai GeneChem, Co., Ltd.) and the appropriate amount of lentivirus (Shanghai GeneChem, Co., Ltd.) were added to 1 ml serum-free RPMI-1640 medium. The amount of lentivirus added to each well (μl) was calculated as follows; multiplicity of infection (MOI) x number of cells/titer (TU/ml) x1,000, where the MOI value was set to 10. The infection medium was replaced with fresh supplemented RPMI-1640 medium following culturing for 12 h. The cells were further cultured for 48 h, after which the cells were observed under a fluorescence microscope. The infection efficiency was >95%.

MTT assay. The cells were digested, and a 5x10^3-1x10^4 cells/ml cell suspension was prepared, of which, 100 μl was added to each well of the 96-well cell culture plate. The seeded cells were cultured for 24 h. 4T-1/IRR cells were treated with different concentrations of R428, and then the lethal IC_{50} dose was calculated. To investigate the role of Axl played in the radioresistance of TNBC cells, the 4T-1/IRR cells were treated with R428, infected with NC or Axl siRNA lentivirus, respectively, and then irradiated with 0 or 4 Gy X-rays; 4 Gy X-ray was regarded as the most suitable dose for the viability test, as it brought about a decrease in cell viability while minimizing the impact of ionizing radiation damage on experimental results. The cell viability was measured using MTT assays after 24 and 48 h. In the dark, 20 μl MTT solution (5 mg/ml) (Beijing Solarbio Science & Technology Co., Ltd.) was added to each well, and the cells were incubated for 4 h. The supernatant in each well was discarded and replaced with 150 μl DMSO (Beijing Solarbio Science & Technology Co., Ltd.) to dissolve the formazan. The optical density (OD) values were

measured at 492 nm on a microplate reader. The cell viability was calculated using the following formula: Cell viability (%)=(OD492 value of experimental group/OD492 value of control group) x100%.

Colony formation assay. The cells in the logarithmic growth phase were digested and seeded into six-well plates with gradient densities of 500, 1,000, 2,000, 3,000, and 4,000 cells/well. The detection of the colony formation ability of 4T-1/IRR cells needs to fit the dose-survival curve, which was derived from a multi-target single-hit model as follows: survival fraction (SF)=1-(1-$exp^{-D/D0}$)^n (24,25). The numbers of colonies formed after 0, 2, 4, 6, or 8 Gy X-ray irradiation are usually used to fit the dose-survival curve. This is a routine operation method for radiobiology tests (24,25). The plates were irradiated with 2, 4, 6, or 8 Gy X-rays, respectively, and subsequently incubated for 10-14 days. Following incubation, the culture supernatant was discarded, and the cells were fixed at room temperature for 20 min with methanol and stained at room temperature for 30 min with crystal violet staining solution. The SF was calculated according to the following formula: SF=number of colonies/(number of inoculated cells x plating efficiency). The number of colonies with >50 cells was counted under a inverted microscope (Olympus Corporation; magnification, x40). The dose-survival curve was derived from a multi-target single-hit model as follows:

SF=1-(1-$exp^{-D/D0}$)^n; where D is the radiation dose (Gy), D_0 is the average lethal dose, Dq is the quasi-domain dose, and N is the extrapolation. The sensitization enhancing ratio (SER) was calculated as follows: D_0 of the treatment group/D_0 of the control group.

Mouse TNBC 4T-1/IRR cell xenografts. The female 5-week-old BALB/c mice were purchased from Shanghai SLAC Laboratory Animal Co., Ltd. The mice were housed under standard laboratory conditions (25±1˚C with 12-h light-dark cycle) and given access to sterilized food and water. The mice were treated in accordance with the ARRIVE guidelines, the UK Animals (Scientific Procedures) Act, 1986, and associated guidelines (26). The cells in each group were inoculated subcutaneously into the right posterior flank of BALB/c mice. A total of 1x10^6 cells suspended in 200 μl PBS were subcutaneously injected into the right posterior flank of the BALB/c mice. Each group consisted of five mice. The length and width of the transplanted tumors were measured every 5 days, and then the tumor volume was calculated using the formula: Volume (mm^3)=length x $width^2$ (mm^2)/2. The maximum diameter of the tumor did not exceed 15 mm. The Small Animal Radiation Research Platform (SARRP; Xstrahl) was used to provide a single dose of 6 Gy 220 KV X-ray irradiation. Intratumoral injection with R428 was used to inhibit the Axl expression of the transplanted tumors. The volume of the transplanted tumor was calculated to generate the growth curve. The mice were sacrificed 20 days after irradiation, and the transplanted tumor was completely removed. Mice were anesthetized with 1% sodium pentobarbital (50 mg/kg) by intraperitoneal injection prior to radiotherapy. The mice were euthanized by cervical dislocation after anesthetization with 1% sodium pentobarbital (50 mg/kg) through intraperitoneal injection. The death of animals was confirmed by a lack of heartbeat, breathing, dilation of the pupils, and nerve reflexes.

Wound healing assay. Wound healing assays were used to assess the migratory ability of tumor cells. Cells were seeded into 6-well plates, treated as described above, and cultured to 80-90% confluency, typically 24 h. The monolayers were scratched using a 200 μl sterile pipette tip and washed with PBS to discard the floating and detached cells. Then, fresh serum-free RPMI-1640 medium was added, and the cells were further cultured. The cells were observed, and images were taken at 0 and 48 h to measure the wound closure distance. The wound closure rates were calculated as follows: (Wound distance of cells after 48 h/wound distance of initial scratch) x100.

Transwell invasion assay. The invasive ability of the cells was assessed using 24-well Matrigel-coated Transwell chambers with 8 μm pore-size membranes (Corning Inc.). A total of 5x10^4/ml cells from each group in serum-free medium were added to the upper chamber. The inserts were pre-coated with 50 μl Matrigel (BD Biosciences) diluted with serum-free RPMI-1640 medium at a ratio of 1:8. In the bottom chamber, 500 μl medium supplemented with 20% FBS was added. After incubation for 48 h, the Matrigel and cells in the upper chambers were removed. The cells that had invaded to the lower chambers were fixed at room temperature for 20 min with 4% paraformaldehyde, stained at room temperature for 30 min with crystal violet, and imaged under a light microscope (Olympus Corporation; magnification, x200).

Immunofluorescence analysis. The rapid phosphorylation of histone H2AX at serine 139 (γH2AX) can be detected by immunofluorescence as DNA double-stranded breaks (DSBs) induced by ionizing radiation. Cells cultured and treated on sterile cell culture slides in 24-well plates, were fixed with 3.7% paraformaldehyde at room temperature for 20 mins, permeabilized with 0.5% Triton X-100, blocked with 1% BSA at room temperature for 2 h, and incubated with an anti-γH2AX antibody (cat. no. ab22551; 1:1,000; Abcam) at 4˚C overnight. Subsequently, the cells were washed and incubated with a TRITC-conjugated anti-rabbit secondary antibody (cat. no. ab6786; 1:1,000; Abcam), followed by counterstaining with DAPI (Beyotime Institute of Biotechnology) at room temperature for 5 mins to mark the nucleus. The immunofluorescence-stained slices were observed and imaged using a fluorescence microscope. The mean number of γH2AX foci per nucleus was quantified in each group.

Western blotting. Cells were lysed in lysis buffer (Thermo Fisher Scientific, Inc.) containing phosphatase inhibitors (Thermo Fisher Scientific Inc.) and PMSF (Thermo Fisher Scientific Inc.). The proteins were loaded on an 10% SDS gel, resolved using SDS-PAGE, and transferred to PVDF membranes (MilliporeSigma). Subsequently, the membranes were blocked with 5% skimmed milk, incubated with primary antibodies against pPI3K (cat. no. ab182651; 1:200; Abcam),

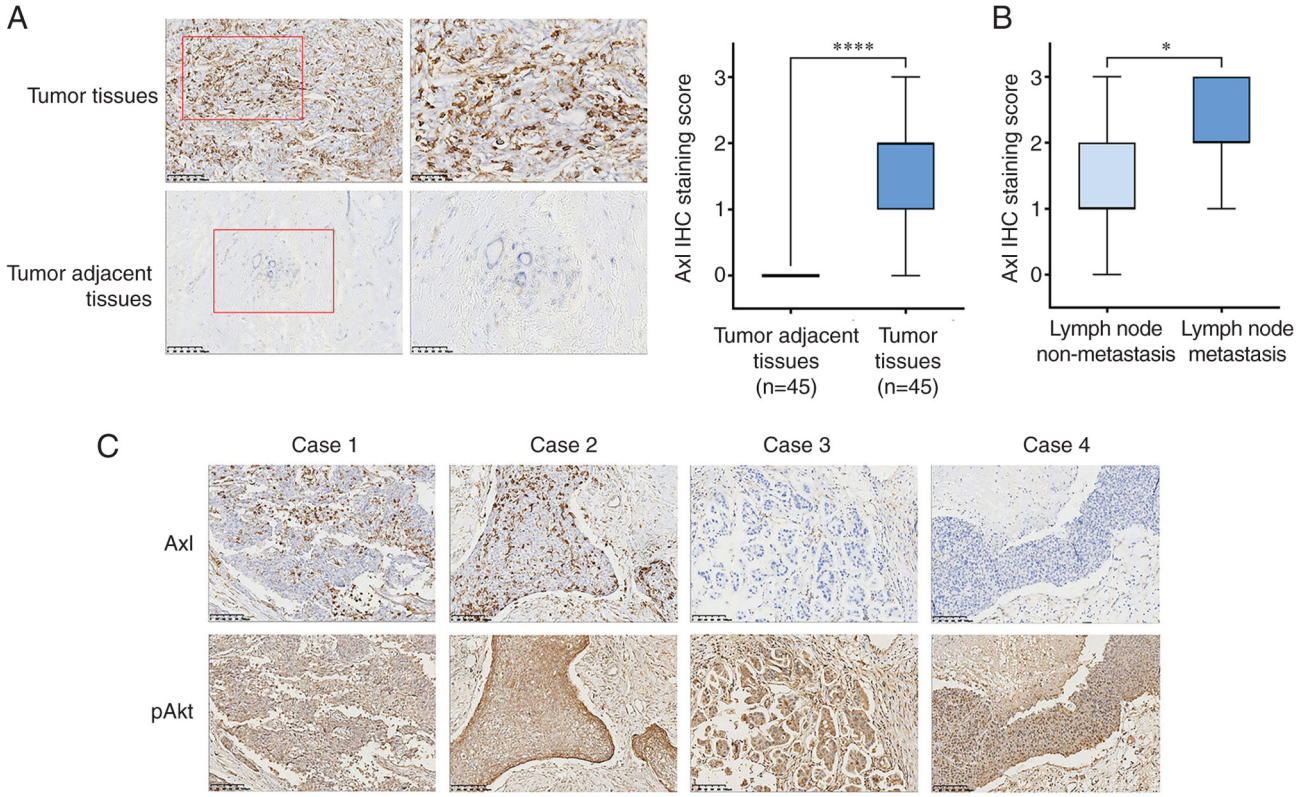

Figure 1. Immunohistochemical analysis of tumor tissues in TNBC patients. (A) Axl expression in TNBC and adjacent tissues. Scale bars, 50 and 100 μm. (B) Correlation analysis between Axl expression and lymph node metastasis. (C) Axl and pAkt expression in TNBC tissues. Scale bar, 100 μm. *P<0.05, ****P<0.0001. TNBC, triple-negative breast cancer.

PI3K (cat. no. ab191606; 1:1,000; Abcam), pAxl (cat. no. 96453; 1:1,000; Cell Signaling Technology, Inc.), Axl (cat. no. ab215205; 1:1,000; Abcam), pAkt (cat. no. ab81283; 1:2,000; Abcam), Akt (cat. no. ab38499; 1:1,000; Abcam), mTOR (cat. no. ab2732; 1:2,000; Abcam), PTEN (cat. no. ab32199; 1:5,000; Abcam), or GAPDH (cat. no. ab8245; 1:2,000; Abcam), followed by incubation with the relevant horseradish peroxidase-conjugated secondary antibody (anti-Rabbit; cat. no. ab205718; anti-Mouse: cat. no. ab6789; Abcam). GAPDH was used as the internal control. Signals were visualized using a Laser Holographic imager (Azure Biosystems).

Statistical analysis. Graph Pad Prism version 5.0 (GraphPad Software, Inc.) and SPSS version 20.0 (IBM Corp.) were used to analyze the data. A Mann-Whitney U test was applied to analyze the clinical data of the TNBC patients. A one-way ANOVA with post hoc Bonferroni's multiple comparison corrections was used to compare the differences between groups *in vitro* or *in vivo*. Data are presented as the mean ± standard deviation. *P<0.05 was considered to indicate a statistically significant difference. The multi-target single-hit model was used to fit the dose-survival curves. The ability of a radiation sensitizer is represented by the SER. SER is the ratio between the radiation dose that achieves a certain effect in the absence of the sensitizer and the radiation dose that achieves the same effect in the presence of the sensitizer. SER >1 was considered to be indicative of a radiation sensitization effect, whereas an SER <1 was considered to indicate a radiation-resistant effect.

Results

Axl and pAkt expression in TNBC tissues. The results of immunohistochemical staining showed that the Axl protein was primarily expressed in the cytoplasm of TNBC cells, although some expression was seen in the nucleus (Fig. 1A). The positive expression rate of Axl in 45 TNBC cases was 88.9% (40/45), of which 26 cases were ++ - +++, while that in the adjacent tissues was 0%. It was thus hypothesized that Axl may play an important role in the occurrence and development of TNBC.

As shown in Fig. 1B, further analysis of the patients' clinicopathological characteristics showed that 16 (35.56%) of 45 TNBC patients had positive axillary lymph node (ALN) metastasis, and Axl expression in the TNBC cases with ALN metastasis was significantly higher than that without lymph node metastasis (P<0.05). pAkt expression was found to be widely distributed in the cytoplasm of tumor cells (Fig. 1C), and the positive expression rate was 100% (45/45). Therefore, it was concluded that the expression of Axl was upregulated in the majority of TNBC patients, and the PI3K/pAkt signaling pathway was an important molecular signaling pathway that modulated the biological processes in TNBC.

Influence of ionizing radiation on the expression of pAxl and its downstream signaling molecules in 4T-1 cells. The expression levels of pAxl, Axl, and the downstream signaling pathway molecules including pPI3K, PI3K, pAkt, Akt, mTOR, and PTEN in 4T-1 cells were detected after 0, 24, 48 ,and

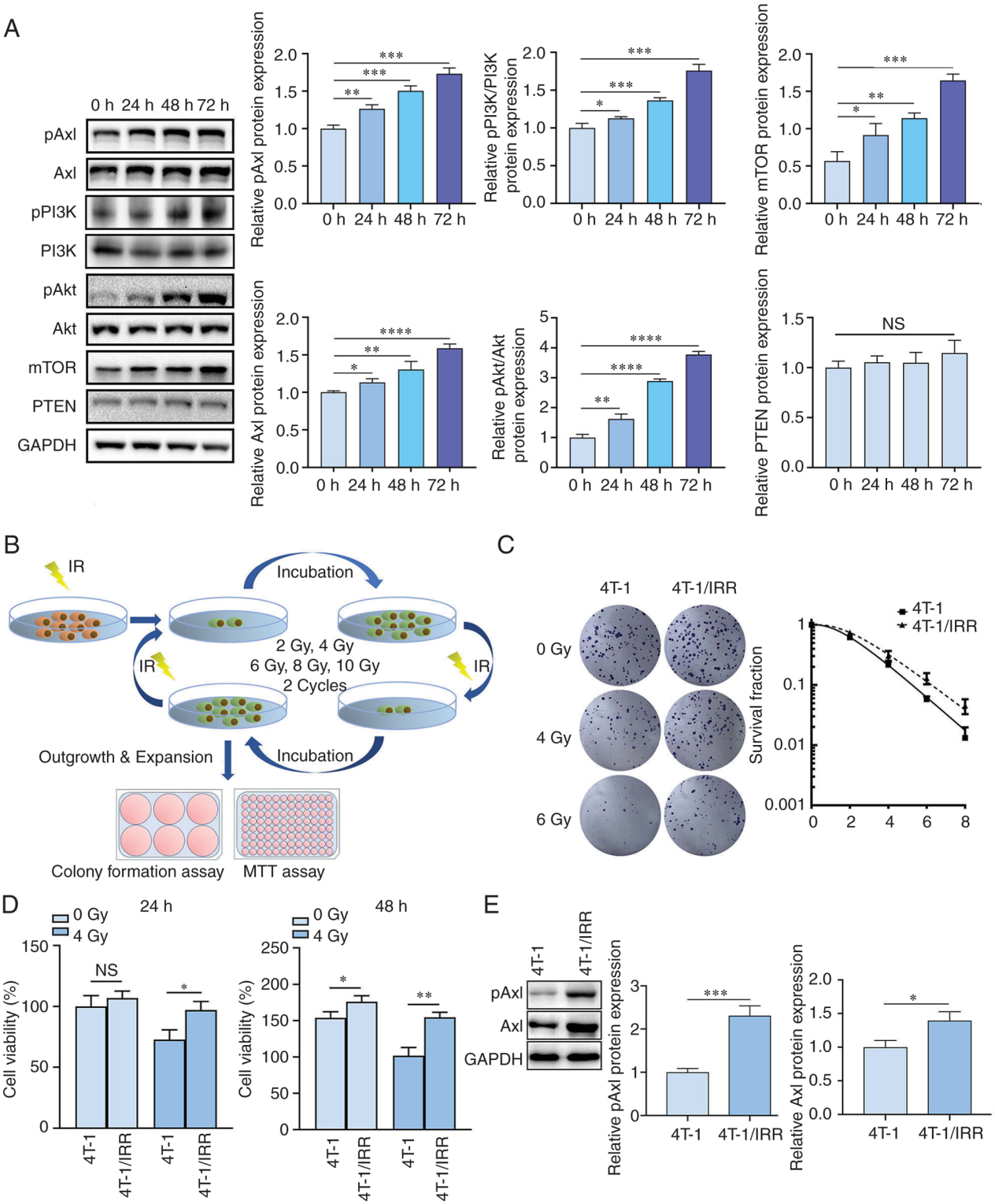

Figure 2. Establishment and identification of ionizing radiation-resistant mouse TNBC 4T-1/IRR cells. (A) pAxl, Axl, pPI3K, PI3K, pAkt, Akt, mTOR, and PTEN expression in 4T-1 cells at different times following irradiation. (B) The construction process of 4T-1/IRR cells using a gradient irradiation method. The (C) colony formation rate and (D) viability of 4T-1/IRR cells was increased. (E) pAxl and Axl expression in 4T-1/IRR cells. *P<0.05, **P<0.01, ***P<0.001, ****P<0.0001. NS, not significant; IRR, ionizing radiation resistance; TNBC, triple-negative breast cancer.

72 h after 2 Gy X-ray irradiation (Fig. 2A), respectively. The results showed that the protein expression levels of pAxl, Axl, pPI3K, pAkt, and mTOR increased gradually as the irradiation time increased. This suggested that in 4T-1 cells, a series of signaling cascades were initiated after irradiation to protect against and gradually repair ionizing radiation damage.

Verification of ionizing radiation-resistant ability for 4T-1/IRR cells. The method used to establish 4T-1/IRR cells is shown in Fig. 2B. Following irradiation with different doses of X-rays, the colony formation rate of 4T-1/IRR cells was notably higher than that of 4T-1 cells (SER=0.8719; Fig. 2C). As shown in Fig. 2D, 24 h after 4 Gy X-ray irradiation, the

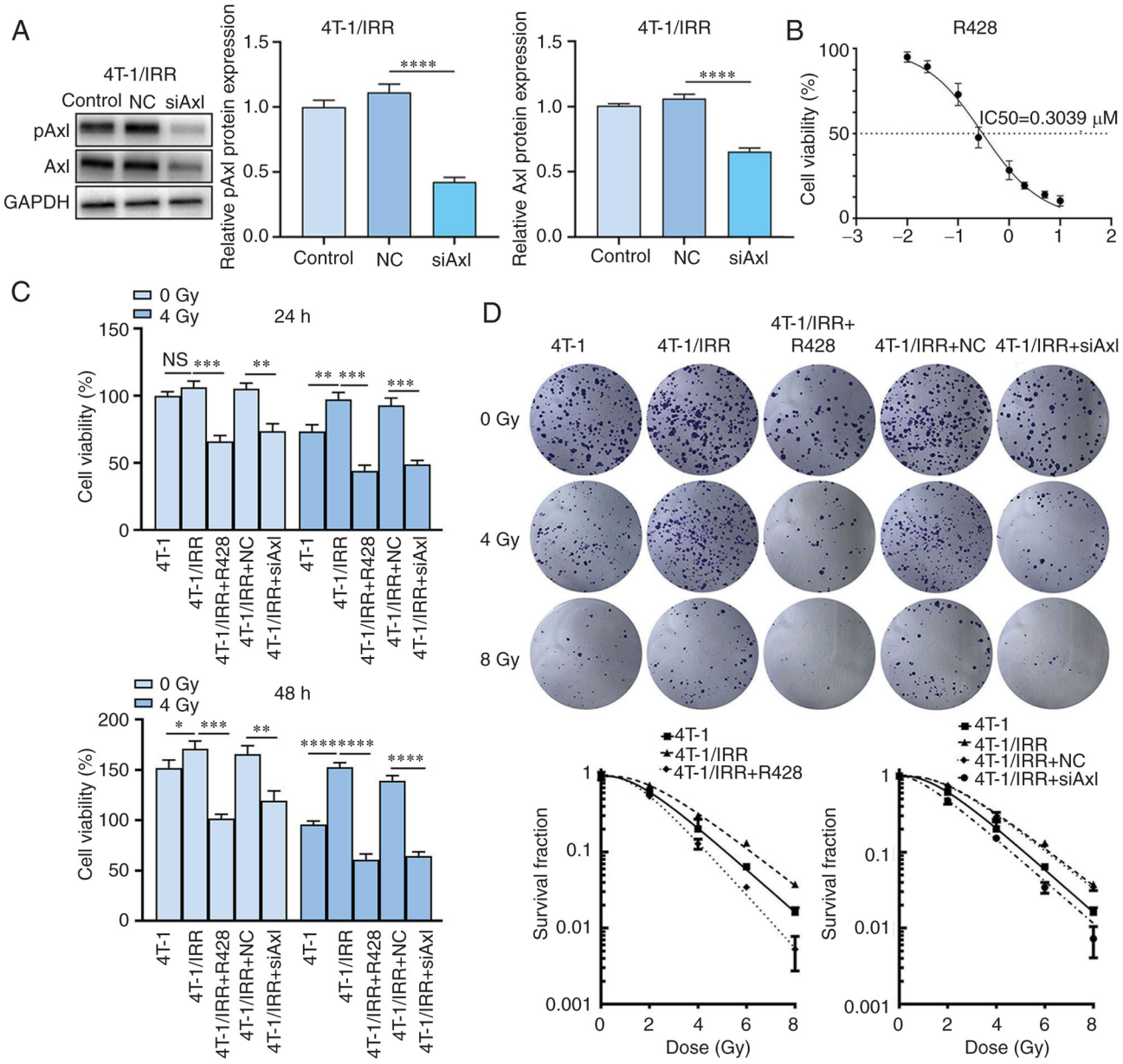

Figure 3. Effects of Axl inhibition and irradiation on 4T-1/IRR cell growth. (A) pAxl and Axl expression was downregulated by siRNA lentivirus infection. (B) Growth curve of 4T-1/IRR cells treated with different concentrations of R428. The effect of combined irradiation with Axl inhibition by R428 treatment and Axl siRNA lentivirus infection on (C) cell viability and (D) colony formation ability of TNBC cells. *P<0.05, **P<0.01, ***P<0.001, ****P<0.0001. NS, Not Significant; NC, negative control; TNBC, triple-negative breast cancer.

viability of 4T-1/IRR cells was significantly higher than that of 4T-1 cells (97.00±7.03% vs. 72.70±8.02%, P<0.05). After 48 h of cell culture, it was found that in the non-irradiation group, the viability of 4T-1/IRR cells was higher than that of 4T-1 cells (175.97±8.28% vs. 154.00±8.19%, P<0.05). A total of 48 h after X-ray irradiation, the difference between the two groups became more significant (154.67±6.76% vs. 101.67±11.24%, P<0.01). The above results confirmed that the colony formation and proliferative ability of 4T-1/IRR cells were significantly higher than that of 4T-1 cells, and it was confirmed that 4T-1/IRR cells had acquired radioresistance. The expression levels of pAxl and Axl in 4T-1/IRR cells were higher than those in 4T-1 cells, particularly for pAxl, suggesting that Axl activation likely participated in the acquisition of radioresistance in TNBC cells (Fig. 2E).

Axl inhibition combined with irradiation significantly reduces the viability of 4T-1/IRR cells. As shown in Fig. 3A, the expression of pAxl and Axl was significantly decreased following Axl siRNA lentiviral infection. In Fig. 3B, the growth curve showed that the median lethal dose (IC_{50}) of R428 for inhibiting 4T-1/IRR cell growth was 0.3039 μM, thus R428 with a drug concentration of 0.3 μM was chosen for the subsequent experiments. As shown in Fig. 3C and Table I, in the unirradiated group, the viability of R428-treated 4T-1/IRR cells after 24 and 48 h was significantly reduced to 62.03 and 59.56% of the 4T-1/IRR cells without R428 treatment. The viability of 4T-1/IRR cells infected with siAxl lentivirus after 24 and 48 h was also significantly decreased to 69.96 and 72.11% of the empty vector infected 4T-1/IRR cells. In the combination treatment groups, the viability of R428 treated 4T-1/IRR

Table I. Cell viability of 4T-1/IRR cells following Axl inhibition[e].

	24 h		48 h	
Group	0 Gy	4 Gy	0 Gy	4 Gy
4T-1	100.00±3.00	88.57±5.03	151.67±8.08	95.67±3.51
4T-1/IRR	106.40±4.54	102.46±5.23[b]	170.80±7.79[a]	152.53±4.57[b]
4T-1/IRR+R428	66.00±4.33[c]	56.57±4.21[c]	101.73±4.28[c]	60.67±5.86[c]
4T-1/IRR+NC	105.20±4.21	99.89±5.41	165.67±8.20	139.10±5.2
4T-1/IRR+siAxl	73.60±5.41[d]	62.97±3.02[d]	119.47±9.53[d]	64.57±4.18[d]

[a]P<0.05, [b]P<0.01 vs. 4T-1; [c]P<0.01 vs. 4T-1/IRR; [d]P<0.01 vs. 4T-1/IRR + NC. [e]Data are presented as the mean % (relative to 4T-1 cells treated with 0 Gy radiation) ± SD. NC, negative control; si, small interfering.

Table II. Colony formation ability of 4T-1/IRR cells following Axl inhibition[a].

Group	0 Gy	2 Gy	4 Gy	6 Gy	8 Gy
4T-1	100.00±7.16	61.46±1.85	20.15±6.92	6.41±0.31	1.62±0.23
4T-1/IRR	100.00±7.33	75.69±1.98	30.25±1.74	13.19±1.13	3.76±0.35
4T-1/IRR+R428	100.00±11.65	54.21±1.56	12.86±1.94	3.45±0.34	0.52±0.25
4T-1/IRR+NC	100.00±8.10	74.54±1.21	29.10±4.15	12.46±1.03	3.49±0.37
4T-1/IRR+siAxl	100.00±8.34	47.58±4.87	15.24±1.11	3.44±0.57	0.73±0.32

[a]Data are presented as the mean % (relative to respective 0 Gy radiation treated cells) ± SD. 4T-1/IRR vs. 4T-1, SER=0.8787; 4T-1/IRR + R428 vs. 4T-1/IRR, SER=1.4104; 4T-1/IRR + siAxl vs. 4T-1/IRR + NC, SER=1.1053. NC, negative control; si, small interfering; SER, sensitization enhancing ratio.

cells after 24 and 48 h was significantly reduced to 53.16 and 35.52% of the 4T-1/IRR cells without any treatment. The viability of 4T-1/IRR cells infected with siAxl lentivirus after 24 and 48 h was significantly decreased to 59.86 and 38.98% of the empty vector infected 4T-1/IRR cells. The above results suggested that ionizing radiation combined with Axl inhibition exhibited an enhanced inhibitory role on the proliferation of radiation-resistant TNBC cells.

Axl inhibition combined with irradiation reduces the colony formation ability of 4T-1/IRR cells. As shown in Fig. 3D and Table II, the colony formation rate of 4T-1/IRR cells was significantly increased when compared with the 4T-1 cells (SER=0.8787). R428-treated 4T-1/IRR cells exhibited a decreased colony formation rate compared with the 4T-1/IRR cells not treated with R428 (SER=1.4104). The colony formation rate of 4T-1/IRR cells was also reduced by siAxl lentivirus infection when compared with the NC lentivirus-infected 4T-1/IRR cells (SER=1.1053). The above results showed that the colony formation ability of 4T-1/IRR cells was promoted when compared with 4T-1 cells, and it could be significantly reduced by Axl inhibition, suggesting that Axl played an important role in the radiation resistance of TNBC cells.

R428 treatment combined with radiotherapy inhibits the rapid growth of 4T-1/IRR cell xenografts. As shown in Fig. 4A, the xenografted mice were fixed in the prone position on the treatment bed, and the analog positioning machine of the SARRP collected the images in 3D. After the planned target area (PTV) was outlined, a vertical X-ray irradiation field above the transplanted tumor on the right hind leg root of the mouse was set up. The center point of the PTV was located at the center of the transplanted tumor. The dose-volume histograms were generated from the treatment planning system of the SARRP, and it was determined that >95% of xenografts achieved 6 Gy X-ray exposure. The subcutaneous xenografts of 4T-1/IRR cells that had not been irradiated grew most rapidly, and this growth was inhibited by R428 treatment (Fig. 4B). In the ionizing radiation treated groups, xenografts were locally irradiated with 6 Gy X-rays, the xenografts of the 4T-1/IRR cells were found to be resistant to ionizing radiation compared with that of 4T-1 cells. R428 treatment could also interrupt the radioresistance of 4T-1/IRR cell xenografts (P<0.01). The tumor volumes of xenografts in the combination treatment group were slightly smaller than that of the tumors treated with R428 alone, but the difference was not significant (P=0.1366).

Axl inhibition combined with irradiation reverses the increase in the migratory capacity of 4T-1/IRR cells. As shown in Fig. 5A, the wound closure rate of 4T-1/IRR cells was 64.77±1.29%, while that of the 4T-1 cells was 48.44±0.83% (P<0.0001). After treatment with R428, the wound closure rate of 4T-1/IRR cells decreased to 31.88±2.91%. The wound closure rate of the 4 Gy X-ray irradiated 4T-1 cells was 13.78±0.43%, while that of

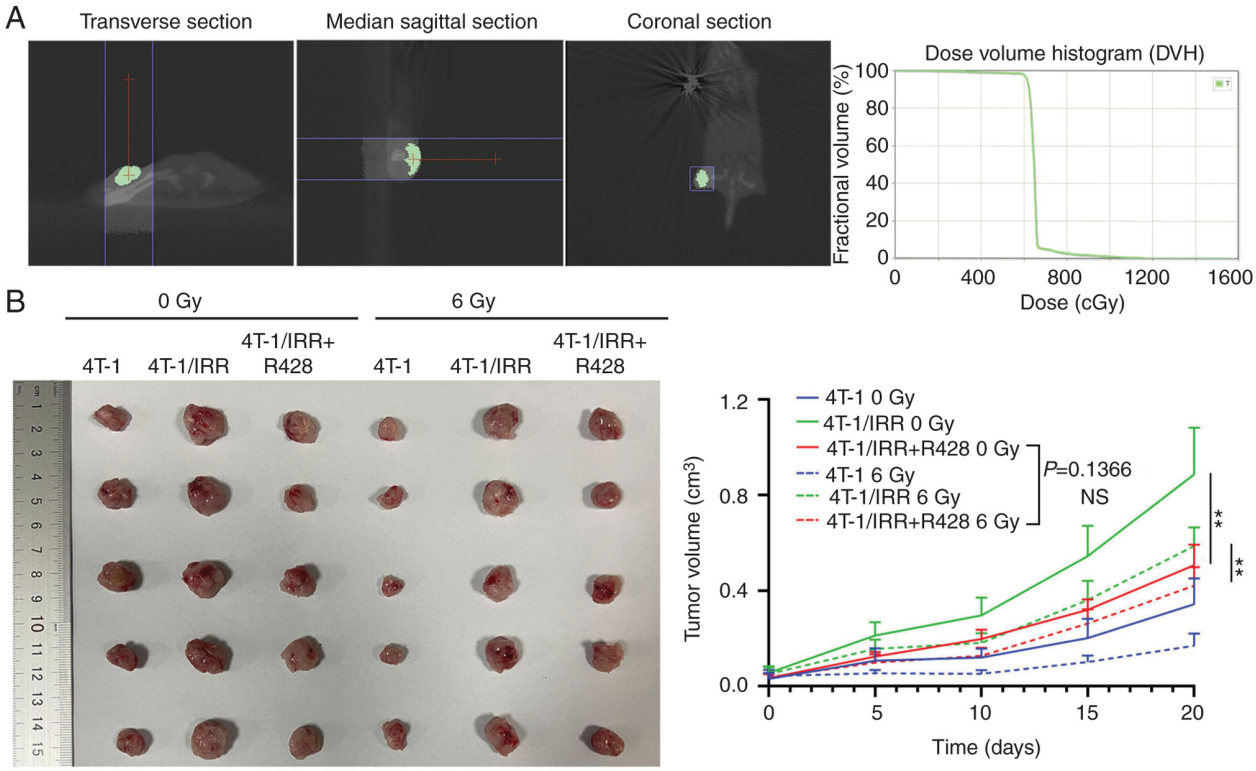

Figure 4. 4T-1/IRR cell xenograft growth is inhibited by R428 treatment combined with SARRP radiotherapy. (A) Irradiation fields and dose-volume histograms for TNBC xenografts in mice. (B) The effect of R428 on the xenograft growth of 4T-1/IRR cells. **P<0.01. NS, Not Significant; TNBC, triple-negative breast cancer; SARRP, small animal radiation research platform.

irradiated 4T-1/IRR cells was 54.30±0.92%. The R428 treatment reduced the wound closure rate of irradiated 4T-1/IRR cells to 16.15±2.09% (P<0.0001). The wound closure rate was 58.98±3.22% in NC lentivirus-infected 4T-1/IRR cells, while it was 26.66±1.65% in siAxl lentivirus-infected 4T-1/IRR cells (P<0.001). After 4 Gy X-ray irradiation, the wound closure rate of 4T-1/IRR cells infected with the empty vector lentivirus was 51.41±1.75%, and it was reduced to 22.45±0.60% after siAxl lentivirus infection (P<0.0001). The above results indicated that the 4T-1/IRR cells exhibited increased migratory capacity, and this increase migratory capacity was dependent on Axl.

Axl inhibition combined with irradiation reverses the increase in the invasive ability of 4T-1/IRR cells. The number of cells that invaded through Matrigel and reached the lower chamber of the chamber was counted to evaluate the invasive ability of tumor cells. As shown in Fig. 5B, the number of invasive 4T-1/IRR cells per field increased to 1.86x that of the 4T-1 cells, and this was decreased to 47.55% in 4T-1/IRR cells treated with R428 compared with the untreated 4T-1/IRR cells (P<0.01). After 4 Gy X-ray irradiation, the invasion of 4T-1/IRR cells was 2.02x that of the 4T-1 cells, and this was decreased to 19.28% in 4T-1/IRR cells treated with R428 compared with the untreated 4T-1/IRR cells (P<0.01). The invasion of siAxl lentivirus-infected 4T-1/IRR cells was reduced to 37.42% of the NC lentivirus-infected 4T-1/IRR cells. After 4 Gy X-ray irradiation, the invasive potential of siAxl lentivirus-infected 4T-1/IRR cells per field was reduced to 20.99% of the NC lentivirus-infected 4T-1/IRR cells (P<0.01). These results indicated that the ability of 4T-1/IRR cells to invade and metastasize from the primary site to distant organs and tissues was also significantly increased, which was associated with the increased expression of Axl.

Axl inhibition reduces ionizing radiation-induced DSBs in 4T-1/IRR cells. The number of γH2AX foci in each group of cells was found to reach a peak 1 h after 2 Gy X-ray irradiation (Fig. 5C), and in 4T-1/IRR cells, the number of foci was notably reduced compared with the 4T-1 cells (54.67±11.23 vs. 95.33±6.51, P<0.01), suggesting that DNA damage in 4T-1/IRR cells was notably reduced. Following treatment of 4T-1/IRR with R428, the degree of ionizing radiation-induced DSBs increased (81.00±7.55 vs. 54.67±11.23, P<0.01). The number of γH2AX foci also increased in siAxl lentivirus-infected 4T-1/IRR cells when compared with that of the NC lentivirus-infected 4T-1/IRR cells (74.33±6.11 vs. 55.0±7.55, P<0.01). The above results demonstrated that the 4T-1/IRR cells exhibited significantly less DNA damage than the 4T-1 cells following irradiation, and the activation of Axl likely protected cells from ionizing radiation-induced DNA damage. That is, the downregulation of Axl expression/activity aggravated DNA damage in 4T-1/IRR cells.

PI3K/pAkt/mTOR pathway activation by Axl phosphorylation is involved in the radioresistance of 4T-1/IRR cells. siAxl lentivirus infection of 4T-1/IRR cells resulted in a significant reduction in pAxl and Axl expression. The expression levels of the downstream signaling molecules pPI3K, pAkt, and mTOR were also decreased, although PTEN expression was not altered (Fig. 6). These results indicated that pAxl modulated

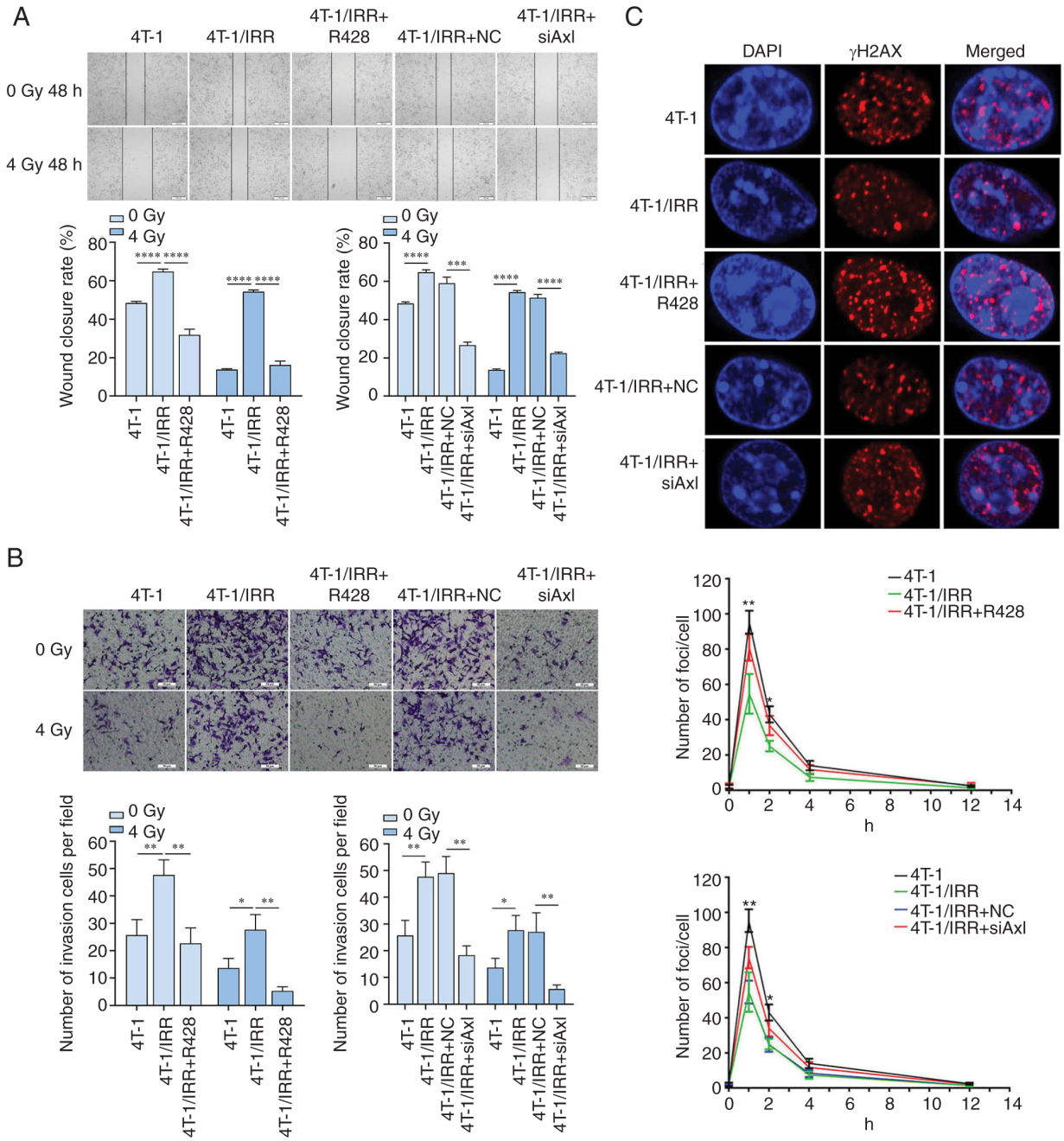

Figure 5. The metastatic ability and DNA repair ability of 4T-1/IRR cells were significantly reduced by combination therapy with Axl inhibition and radiotherapy. (A) migratory capability (scale bar, 400 μm), (B) invasive capability (scale bar, 50 μm), and (C) DNA double-stranded breaks following Axl inhibition in 4T-1/IRR cells and irradiation. *P<0.05, **P<0.01, ***P<0.001, ****P<0.0001. NC, negative control; si, small interfering.

various biological functions of tumor cells through the activation of the downstream PI3K/pAkt/mTOR signaling pathway. R428 also suppressed the expression levels of pAxl, Axl, and the downstream signaling molecules pPI3K, pAkt, and mTOR in 4T-1/IRR cells (Fig. 7). Ionizing radiation-induced the upregulation of pAxl expression in 4T-1 cells, and 4T-1/IRR cells exhibited higher pAxl expression levels. The expression levels of the downstream signaling molecules pPI3K, pAkt, and mTOR were accordingly upregulated, which may be a defense mechanism of tumor cells against ionizing radiation damage. Blocking pAxl activity by R428 or siRNA lentivirus infection enhanced the radiosensitivity of 4T-1/IRR cells, likely through intercepting the PI3K/pAkt/mTOR signal cascade.

Discussion

RTKs are important growth factor receptors present on the cell surface, and they play critical roles in the survival and proliferation of breast and other epithelial cells. The dysregulation of RTKs was found to be closely associated with the occurrence of breast cancer, and the increased expression of RTKs was associated with the enhanced invasiveness of breast cancer, as well as decreased overall survival (OS) and disease-free survival (DFS) (27,28). Currently, the prognosis of TNBC is still poor due to the lack of targeted therapeutic drugs; RTK inhibition may thus have significant potential for the treatment of TNBC.

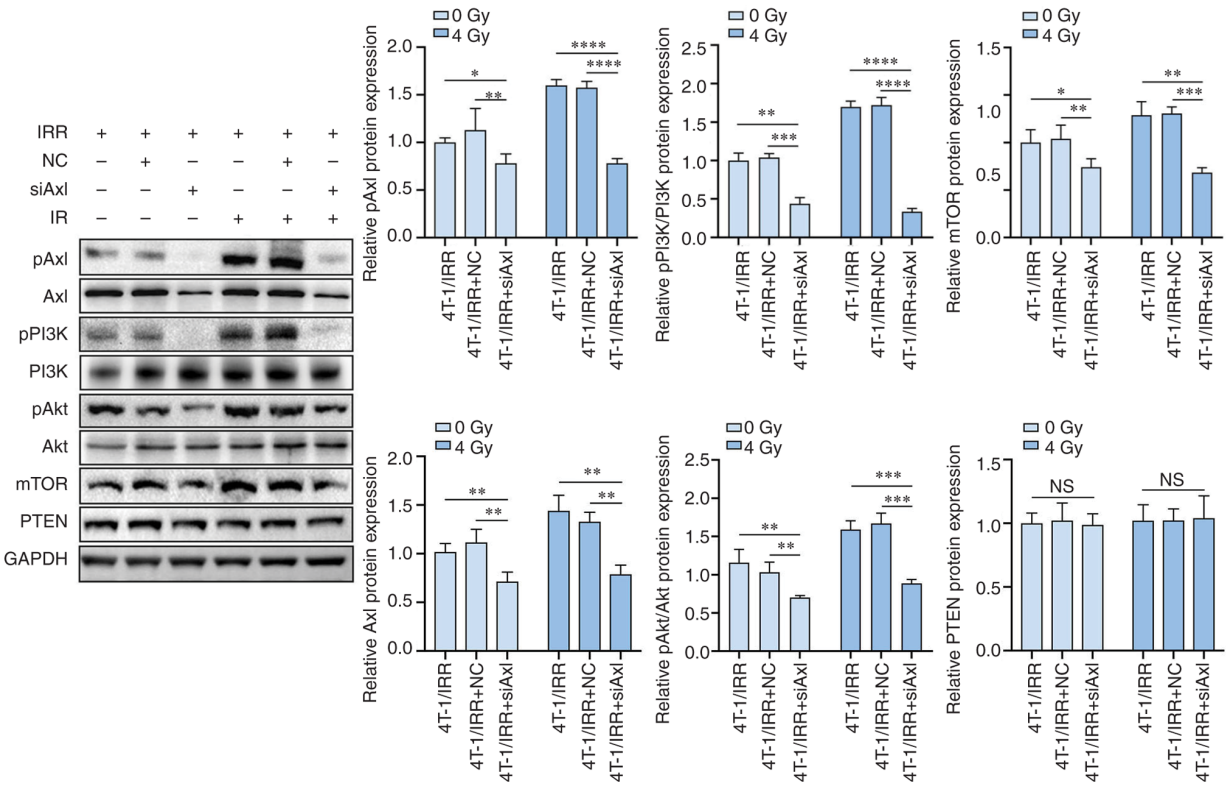

Figure 6. The protein expression levels of pAxl, Axl, pPI3K, PI3K, pAkt, Akt, mTOR, and PTEN in TNBC cells with Axl siRNA lentivirus infection and radiotherapy combination therapy. *P<0.05, **P<0.01, ***P<0.001, ****P<0.0001. TNBC, triple-negative breast cancer.

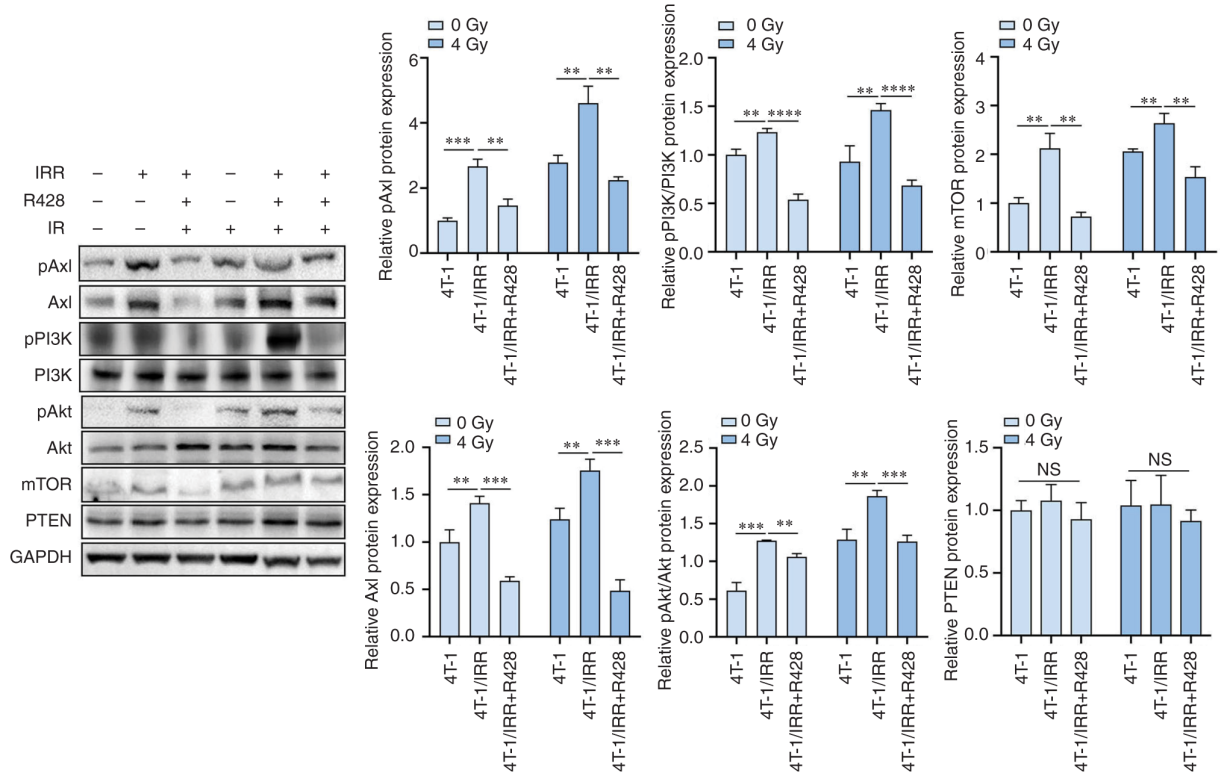

Figure 7. The protein expression levels of pAxl, Axl, pPI3K, PI3K, pAkt, Akt, mTOR, and PTEN in TNBC cells following a combination of R428 treatment and radiotherapy. **P<0.01, ***P<0.001, ****P<0.0001. TNBC, triple-negative breast cancer.

Axl is a member of the Tyro-Axl-MER (TAM) family of RTKs, which regulate a variety of cellular biological processes, including cell survival, proliferation, autophagy, migration, angiogenesis, platelet aggregation, and natural killer cell

differentiation. A meta-analysis performed by Zhang *et al* (29) demonstrated that high expression of Axl was associated with a poorer OS in patients with hepatocellular carcinoma, esophageal cancer, and non-small cell lung cancer. Tanaka *et al* (30) reported that the co-expression of Axl and Vimentin in breast cancer tissues indicated the shortened OS of patients. Bottai *et al* (15) found that the expression of Axl was elevated in the tumor tissues of breast cancer patients with lymph node metastasis or distant metastasis; however, it was not associated with tumor size or clinical stage. Gjerdrum *et al* (31) reported that Axl expression, tumor diameter, histological grade, and lymph node status were negative independent prognostic factors for breast cancer. Axl expression in the metastatic tissues was significantly increased when compared with the primary tumor tissues, indicating that Axl expression was closely associated with distant metastasis of breast cancer. In the present study, it was found that the expression levels of Axl in TNBC tissues were significantly higher than that in adjacent tissues, and Axl expression in the tumor tissues of patients with lymph node metastasis was significantly higher than that of patients without lymph node metastases. The above results indicated that Axl expression may be closely associated with the occurrence and metastasis of TNBC.

According to previous studies, Axl expression was upregulated in TNBC cell lines and was associated with a poor clinical prognosis of breast cancer (32). Downregulation of Axl can effectively prevent the highly metastatic phenotype breast cancer cells migrating from the primary tumor to distant organs and tissues in animal models of breast cancer while improving the OS rate of the animals (33). Abdel-Rahman *et al* (34) found that the upregulation of Axl in breast cancer cells was negatively associated with the expression of the epithelial cell marker E-cadherin. Downregulation of Axl reduced the invasion and migration ability of breast cancer cells. Another study confirmed that Axl activation was able to induce the activation of the NF-κB signaling pathway, promote the expression of MMP-9, and then led to the enhancement of the invasion and migration of breast cancer cells (19). A study by Holland *et al* (35) demonstrated that the downregulation of Axl significantly inhibited the growth of tumors in a nude mouse xenograft model, indicating that Axl also participated in the proliferation and viability of breast cancer cells. Therefore, the detection and targeted therapy of Axl may serve as an important direction for breast cancer treatment.

In the present study, the 4T-1/IRR cells exhibited significantly enhanced cell viability, colony formation ability, DNA injury repair capacity, and invasive and migratory ability. Axl expression was found to be increased in 4T-1/IRR cells, suggesting the possibility that Axl plays an important role in the resistance to ionizing radiation. Axl inhibition reversed the radioresistance of 4T-1/IRR cells, as shown by the attenuated cell viability and colony formation ability, the increase in DNA damage, and the reduction of cell invasion and migration. *In vivo*, it was observed that the growth rate of the transplanted tumor in the mice implanted with 4T-1/IRR cells was notably faster than that of the 4T-1 cells. Combination treatment with R428 and radiotherapy significantly reduced the growth rate of the 4T-1/IRR cell-formed tumors in the mouse model, consistent with the results *in vitro*. The toxicity of combination treatment to animal models exhibits no difference when compared to other groups. The main reasons include: i) The small animal radiation research platform (SARRP) was applied to precisely administer radiotherapy of the tumor-bearing mice; ii) the tumor was implanted in the right posterior flank of BALB/c mice; and iii) the intra-tumoral injection with R428 was the administration pathway. There was relatively little impact on important tissues and organs of the animals. There was no significant difference in weight among groups. The above results showed that Axl played a crucial role in the radioresistance of TNBC. Targeting Axl combined with radiotherapy may thus serve as a potential novel direction for TNBC treatment. However, in the present study, the inhibitory effect of the combination treatment on tumor xenografts did not differ significantly when compared to treatment with R428 alone. This may be explained by the fact the challenges in comparing *in vivo* and *in vitro* experiments; thus, there is a need for further exploration of radiation doses and segmentation of the xenografts; and for improvements in R428 administration methods. In animal experiments and clinical applications, the method of combination therapy also requires further exploration.

According to previous studies, Axl activation in breast cancer induces the activation of multiple downstream signaling transduction pathways, including PI3K/Akt, MAPK, and NF-κB, and thus accelerates various tumor-promoting processes, including cell proliferation, survival, invasion, and angiogenesis (36,37). The PI3K/Akt signaling pathway was involved in the regulation of tumor cell proliferation, survival, metastasis, and EMT in various human malignancies, and it was considered a crucial therapeutic target (38). It has been reported that the activation of the PI3K/Akt signaling pathway led to the overexpression and reduced degradation of Snail, which was an important transcription factor in the EMT process, and ultimately promoted the radioresistance of tumor cells (39). The PI3K/Akt signaling pathway activated by miR-410/PTEN led to the occurrence of EMT and radioresistance of non-small cell lung cancer cells (40). PF-05212384, an inhibitor of PI3K/mTOR, could effectively suppress the PI3K/mTOR signaling pathway and lead to increased sensitivity of head and neck squamous cell carcinoma to ionizing radiation (41). The Akt/mTOR inhibitor everolimus (RAD001) is currently undergoing clinical trials in combination with radiotherapy for the treatment of various malignant tumors, and it may become an effective radiosensitizer (42). The present study showed that Axl expression was notably increased in the 4T-1/IRR cells. The expression of the downstream signaling pathway molecules pAkt and mTOR was simultaneously increased, and significantly downregulated by R428 treatment or siRNA lentivirus infection, indicating that the PI3K/Akt/mTOR signaling pathway was a critical molecular mechanism of TNBC cells resistant to ionizing radiation.

In conclusion, a TNBC cell line resistant to ionizing radiation was established using a gradient irradiation method. *In vitro*, the 4T-1/IRR cells exhibited significantly enhanced radioresistance, and Axl inhibition resulted in increased radiosensitivity in these cells; *in vivo* experiments further confirmed the above results. The PI3K/Akt/mTOR signaling pathway activated by Axl phosphorylation was a critical molecular mechanism of TNBC radioresistance. Axl-targeting therapy

combined with radiotherapy may thus have potential for the management of TNBC.

Acknowledgements

Not applicable.

Funding

The present study was supported by the National Natural Science Foundation of China (grant nos. 81602672 and 81902722) and Medical Health Science and Technology Project of Zhejiang Province (grant nos. 2020KY061, 2021RC041 and 2023KY594).

Availability of data and materials

The datasets used and/or analyzed during the current study are available from the corresponding author on reasonable request.

Authors' contributions

JJ, XL and QG conceived the study. JJ, YD and QG designed the study. YD and MF searched the literature. JJ and YK performed the analysis. JJ, YD, MF, QG and XY performed the experiments. JJ, XL and QG collected the data. JJ wrote the manuscript. XL and QG reviewed and edited the manuscript. JJ, XL and QG confirm the authenticity of all the raw data. All authors have read and approved the final manuscript.

Ethics approval and consent to participate

The present study was approved by the Ethics Committee of Zhejiang Cancer Hospital (Zhejiang, China; approval no, IRB-2020-367). All patients signed informed consent forms prior to tissue collection for storage in the biological sample bank. The Ethics Committee of Zhejiang Cancer Hospital waived the need for informed consent of patients for participation in the present study. The animal experiments were approved by the Animal Ethics Committee of Zhejiang Cancer Hospital (Zhejiang, China; approval no. 2021-11-004).

Patient content for publication

Not applicable.

Competing interests

The authors declare that they have no competing interests.

References

1. Vagia E, Mahalingam D and Cristofanilli M: The landscape of targeted therapies in TNBC. Cancers (Basel) 12: 916, 2020.
2. Jiang MJ, Chen YY, Dai JJ, Gu DN, Mei Z, Liu FR, Huang Q and Tian L: Dying tumor cell-derived exosomal miR-194-5p potentiates survival and repopulation of tumor repopulating cells upon radiotherapy in pancreatic cancer. Mol Cancer 19: 68, 2020.
3. Wang Y, Zhao M, He S, Luo Y, Zhao Y, Cheng J, Gong Y, Xie J, Wang Y, Hu B, *et al*: Necroptosis regulates tumor repopulation after radiotherapy via RIP1/RIP3/MLKL/JNK/IL8 pathway. J Exp Clin Cancer Res 38: 461, 2019.
4. Candas-Green D, Xie B, Huang J, Fan M, Wang A, Menaa C, Zhang Y, Zhang L, Jing D, Azghadi S, *et al*: Dual blockade of CD47 and HER2 eliminates radioresistant breast cancer cells. Nat Commun 11: 4591, 2020.
5. Bai X, Ni J, Beretov J, Wang S, Dong X, Graham P and Li Y: THOC2 and THOC5 regulate stemness and radioresistance in triple-negative breast cancer. Adv Sci (Weinh) 8: e2102658, 2021.
6. Colli LM, Machiela MJ, Zhang H, Myers TA, Jessop L, Delattre O, Yu K and Chanock SJ: Landscape of combination immunotherapy and targeted therapy to improve cancer management. Cancer Res 77: 3666-3671, 2017.
7. Seebacher NA, Stacy AE, Porter GM and Merlot AM: Clinical development of targeted and immune based anti-cancer therapies. J Exp Clin Cancer Res 38: 156, 2019.
8. Trenker R and Jura N: Receptor tyrosine kinase activation: From the ligand perspective. Curr Opin Cell Biol 63: 174-185, 2020.
9. Colavito SA: AXL as a target in breast cancer therapy. J Oncol 2020: 5291952, 2020.
10. Aguilera TA, Rafat M, Castellini L, Shehade H, Kariolis MS, Hui AB, Stehr H, von Eyben R, Jiang D, Ellies LG, *et al*: Reprogramming the immunological microenvironment through radiation and targeting Axl. Nat Commun 7: 13898, 2016.
11. Tang Y, Zang H, Wen Q and Fan S: AXL in cancer: A modulator of drug resistance and therapeutic target. J Exp Clin Cancer Res 42: 148, 2023.
12. Li H, Liu Z, Liu L, Zhang H, Han C, Girard L, Park H, Zhang A, Dong C, Ye J, *et al*: AXL targeting restores PD-1 blockade sensitivity of STK11/LKB1 mutant NSCLC through expansion of TCF1(+) CD8 T cells. Cell Rep Med 3: 100554, 2022.
13. Noronha A, Nataraj NB, Lee JS, Zhitomirsky B, Oren Y, Oster S, Lindzen M, Mukherjee S, Will R, Ghosh S, *et al*: AXL and error-prone DNA replication confer drug resistance and offer strategies to treat EGFR-mutant lung cancer. Cancer Discov 12: 2666-2683, 2022.
14. He R, Song Z, Bai Y, He S, Huang J, Wang Y, Zhou F, Huang W, Guo J, Wang Z, *et al*: Discovery of AXL degraders with improved potencies in triple-negative breast cancer (TNBC) cells. J Med Chem 66: 1873-1891, 2023.
15. Bottai G, Raschioni C, Székely B, Di Tommaso L, Szász AM, Losurdo A, Győrffy B, Ács B, Torrisi R, Karachaliou N, *et al*: AXL-associated tumor inflammation as a poor prognostic signature in chemotherapy-treated triple-negative breast cancer patients. NPJ Breast Cancer 2: 16033, 2016.
16. Han J, Tian R, Yong B, Luo C, Tan P, Shen J and Peng T: Gas6/Axl mediates tumor cell apoptosis, migration and invasion and predicts the clinical outcome of osteosarcoma patients. Biochem Biophys Res Commun 435: 493-500, 2013.
17. Linger RM, Keating AK, Earp HS and Graham DK: TAM receptor tyrosine kinases: Biologic functions, signaling, and potential therapeutic targeting in human cancer. Adv Cancer Res 100: 35-83, 2008.
18. Zhu C, Wei Y and Wei X: AXL receptor tyrosine kinase as a promising anti-cancer approach: Functions, molecular mechanisms and clinical applications. Mol Cancer 18: 153, 2019.
19. Tai KY, Shieh YS, Lee CS, Shiah SG and Wu CW: Axl promotes cell invasion by inducing MMP-9 activity through activation of NF-kappaB and Brg-1. Oncogene 27: 4044-4055, 2008.
20. Rankin EB, Fuh KC, Taylor TE, Krieg AJ, Musser M, Yuan J, Wei K, Kuo CJ, Longacre TA and Giaccia AJ: AXL is an essential factor and therapeutic target for metastatic ovarian cancer. Cancer Res 70: 7570-7579, 2010.
21. Miricescu D, Totan A, Stanescu-Spinu II, Badoiu SC, Stefani C and Greabu M: PI3K/AKT/mTOR signaling pathway in breast cancer: From molecular landscape to clinical aspects. Int J Mol Sci 22: 173, 2020.
22. Park JH, Kim YH, Shim S, Kim A, Jang H, Lee SJ, Park S, Seo S, Jang WI, Lee SB and Kim MJ: Radiation-activated PI3K/AKT pathway promotes the induction of cancer stem-like cells via the upregulation of SOX2 in colorectal cancer. Cells 10: 135, 2021.
23. Seol MY, Choi SH and Yoon HI: Combining radiation with PI3K isoform-selective inhibitor administration increases radiosensitivity and suppresses tumor growth in non-small cell lung cancer. J Radiat Res 63: 591-601, 2022.
24. Yu L, Guo Q, Luo Z, Wang Y, Weng J, Chen Y, Liang W, Li Y, Zhang Y, Chen K, *et al*: TXN inhibitor impedes radioresistance of colorectal cancer cells with decreased ALDH1L2 expression via TXN/NF-κB signaling pathway. Br J Cancer 127: 637-648, 2022.
25. Spring E and Holmberg P: Evaluation of experimental irradiation fractionation with the single-hit, multi-target model. Acta Radiol Ther Phys Biol 7: 297-306, 1968.

26. du Sert NP, Ahluwalia A, Alam S, Avey MT, Baker M, Browne WJ, Clark A, Cuthill IC, Dirnagl U, Emerson M, *et al*: Reporting animal research: Explanation and elaboration for the ARRIVE guidelines 2.0. PLoS Biol 18: e3000411, 2020.
27. Butti R, Das S, Gunasekaran VP, Yadav AS, Kumar D and Kundu GC: Receptor tyrosine kinases (RTKs) in breast cancer: Signaling, therapeutic implications and challenges. Mol Cancer 17: 34, 2018.
28. Itoh T, Hatano R, Horimoto Y, Yamada T, Song D, Otsuka H, Shirakawa Y, Mastuoka S, Iwao N, Aune TM, *et al*: IL-26 mediates epidermal growth factor receptor-tyrosine kinase inhibitor resistance through endoplasmic reticulum stress signaling pathway in triple-negative breast cancer cells. Cell Death Dis 12: 520, 2021.
29. Zhang S, Xu XS, Yang JX, Guo JH, Chao TF and Tong Y: The prognostic role of Gas6/Axl axis in solid malignancies: A meta-analysis and literature review. Onco Targets Ther 11: 509-519, 2018.
30. Tanaka K, Tokunaga E, Inoue Y, Yamashita N, Saeki H, Okano S, Kitao H, Oki E, Oda Y and Maehara Y: Impact of expression of vimentin and Axl in breast cancer. Clin Breast Cancer 16: 520-526, 2016.
31. Gjerdrum C, Tiron C, Høiby T, Stefansson I, Haugen H, Sandal T, Collett K, Li S, McCormack E, Gjertsen BT, *et al*: Axl is an essential epithelial-to-mesenchymal transition-induced regulator of breast cancer metastasis and patient survival. Proc Natl Acad Sci USA 107: 1124-1129, 2010.
32. Zajac O, Leclere R, Nicolas A, Meseure D, Marchiò C, Vincent-Salomon A, Roman-Roman S, Schoumacher M and Dubois T: AXL controls directed migration of mesenchymal triple-negative breast cancer cells. Cells 9: 247, 2020.
33. Leconet W, Chentouf M, du Manoir S, Chevalier C, Sirvent A, Aït-Arsa I, Busson M, Jarlier M, Radosevic-Robin N, Theillet C, *et al*: Therapeutic activity of Anti-AXL antibody against triple-negative breast cancer patient-derived xenografts and metastasis. Clin Cancer Res 23: 2806-2816, 2017.
34. Abdel-Rahman WM, Al-Khayyal NA, Nair VA, Aravind SR and Saber-Ayad M: Role of AXL in invasion and drug resistance of colon and breast cancer cells and its association with p53 alterations. World J Gastroenterol 23: 3440-3448, 2017.
35. Holland SJ, Powell MJ, Franci C, Chan EW, Friera AM, Atchison RE, McLaughlin J, Swift SE, Pali ES, Yam G, *et al*: Multiple roles for the receptor tyrosine kinase axl in tumor formation. Cancer Res 65: 9294-9303, 2005.
36. Jiang C, Cheng Z, Jiang T, Xu Y and Wang B: MicroRNA-34a inhibits cell invasion and epithelial-mesenchymal transition via targeting AXL/PI3K/AKT/Snail signaling in nasopharyngeal carcinoma. Genes Genomics 42: 971-978, 2020.
37. Corno C, Gatti L, Lanzi C, Zaffaroni N, Colombo D and Perego P: Role of the receptor tyrosine kinase axl and its targeting in cancer cells. Curr Med Chem 23: 1496-1512, 2016.
38. Aoki M and Fujishita T: Oncogenic roles of the PI3K/AKT/mTOR axis. Curr Top Microbiol Immunol 407: 153-189, 2017.
39. Lee SY, Jeong EK, Ju MK, Jeon HM, Kim MY, Kim CH, Park HG, Han SI and Kang HS: Induction of metastasis, cancer stem cell phenotype, and oncogenic metabolism in cancer cells by ionizing radiation. Mol Cancer 16: 10, 2017.
40. Yuan Y, Liao H, Pu Q, Ke X, Hu X, Ma Y, Luo X, Jiang Q, Gong Y, Wu M, *et al*: miR-410 induces both epithelial-mesenchymal transition and radioresistance through activation of the PI3K/mTOR pathway in non-small cell lung cancer. Signal Transduct Target Ther 5: 85, 2020.
41. Leiker AJ, DeGraff W, Choudhuri R, Sowers AL, Thetford A, Cook JA, Van Waes C and Mitchell JB: Radiation enhancement of head and neck squamous cell carcinoma by the dual PI3K/mTOR inhibitor PF-05212384. Clin Cancer Res 21: 2792-2801, 2015.
42. Albert JM, Kim KW, Cao C and Lu B: Targeting the Akt/mammalian target of rapamycin pathway for radiosensitization of breast cancer. Mol Cancer Ther 5: 1183-1189, 2006.